

# Role of Interhelical H-Bonds ( $W\alpha 14-T\alpha 67$ and $W\beta 15-S\beta 72$ ) in the Hemoglobin Allosteric Reaction Path Evaluated by UV Resonance Raman Spectroscopy of Site-Mutants

Daojing Wang,<sup>†</sup> Xiaojie Zhao,<sup>†</sup> Tong-Jian Shen,<sup>‡</sup> Chien Ho,<sup>‡</sup> and Thomas G. Spiro<sup>\*,†</sup>

Contribution from the Department of Chemistry, Princeton University, Princeton, New Jersey 08544, and Department of Biological Sciences, Carnegie Mellon University, 4400 Fifth Avenue, Pittsburgh, Pennsylvania 15213

Received June 28, 1999. Revised Manuscript Received September 8, 1999

**Abstract:** Hemoglobin residues Thr $\alpha 67$  and Ser $\beta 72$  have been mutated to Val and Ala, respectively, to test the hypothesis that tertiary H-bonds involving these residues play a key role in the allosteric reaction path between the R and the T state. The H-bonds are donated by the indole side chains of Trp $\alpha 14$  and Trp $\beta 15$ ; they bridge the outer A helices to the inner E helices, which line the distal side of the heme pocket. The mutants fold properly (CD measurements) and form native-like T state contacts, as revealed by UVRR (RR = resonance Raman) difference spectra between deoxyHb and HbCO, and by the Fe–N (histidine) stretching band in the visible RR spectra of deoxyHb. However, the UVRR intensity of tryptophan bands is diminished in the mutants. This is the expected effect of H-bond elimination, because H-bonding shifts the tryptophan excitation profiles to longer wavelengths, raising the intensity at 229 nm, the wavelength employed in this study. Consistent with this interpretation, the intensity loss for the W3 band is found exclusively at 1558 cm<sup>-1</sup>, the position of Trp $\alpha 14$  and Trp $\beta 15$ , and not at 1548 cm<sup>-1</sup>, the position of the interfacial residue Trp $\beta 37$ . The intensity loss is greater for T $\alpha 67V$  than for S $\beta 72A$ , consistent with crystallographic data showing a shorter N $\cdots$ O distance for the H-bond from Trp $\alpha 14$  than from Trp $\beta 15$ . The H-bond augmentation of the W3 intensity is calculated to be almost a factor of 2 greater for the former than the latter. UVRR difference spectra obtained 150 ns after photolysis of HbCO reveal negative Tyr and Trp bands for the mutants which are similar to those obtained for native Hb, and are attributed to the first protein intermediate on the allosteric reaction path, R<sub>deoxy</sub>. However, the Trp intensity loss is diminished for the mutants, supporting the hypothesis that the R<sub>deoxy</sub> Trp signals arise from weakening of the Trp $\alpha 14$  and Trp $\beta 15$  H-bonds, as a result of increased separation between the A and E helices. This separation is proposed to result from rotation of the EF “clamshell” resulting from F helix displacement away from the heme plane, due to the Fe displacement upon deligation, and E helix motion toward the heme plane as the ligand departs the heme pocket.

## Introduction

While the end states of the allosteric transition in hemoglobin (Hb) are the well-established R and T structures,<sup>1</sup> the reaction path has not been defined and remains a subject of great interest. As part of a continuing program to trace this path with the aid of time-resolved vibrational spectroscopy,<sup>2–6</sup> we have examined the effects of mutating residues Thr $\alpha 67$  and Ser $\beta 72$ , which are involved in key tertiary H-bonds. These mutants were designed to test a specific hypothesis<sup>3,4,6</sup> about the first protein motion detectable by ultraviolet resonance Raman (UVRR) spectroscopy, when Hb is induced to undergo the R to T transition by flash photolysis of the CO adduct, HbCO. This motion is

proposed to involve displacement of the helices, E and F, which sandwich the heme prosthetic group (Figure 1). These displacements would weaken H-bonds connecting the E helix to the A helix, on one hand, and the F helix with the H helix on the other. In our model of the allosteric reaction coordinate,<sup>4,6</sup> these H-bonds are subsequently reformed by following motions of the A and H helices, which serve to move the N and C termini into positions from which they establish the intersubunit salt-bridges that stabilize the T structure.<sup>8</sup>

UVRR spectroscopy can monitor the E–A and F–H helix separations, because the interhelical H-bonds involve aromatic residues. The H-bonds connecting the F and H helices are from the penultimate tyrosine residues,  $\alpha 140$  and  $\beta 145$  to the main chain carbonyl groups of valine residues  $\alpha 93$  and  $\beta 98$ , while the H-bonds connecting the E and A helices are from the tryptophan residues  $\alpha 14$  and  $\beta 15$  to the hydroxyl side chains of Thr $\alpha 67$  and Ser $\beta 72$  (Figure 1). When tyrosine or tryptophan are H-bond donors, the UVRR excitation profiles are red-shifted,<sup>2</sup> reflecting stabilization of the resonant excited states. As a result, their UVRR intensity is increased for excitation at 229 nm, the wavelength used in our studies. Thus, weakening

\* To whom correspondence should be addressed.

<sup>†</sup> Princeton University.

<sup>‡</sup> Carnegie Mellon University.

(1) Perutz, M. *Mechanism of Cooperativity and Allosteric Regulation in Proteins*; Cambridge University Press: Cambridge, 1990.

(2) Rodgers, K. R.; Su, C.; Subramaniam, S.; Spiro, T. G. *J. Am. Chem. Soc.* **1992**, *114*, 3697.

(3) Rodgers, K. R.; Spiro, T. G. *Science* **1994**, *265*, 1697.

(4) Jayaraman, V.; Rodgers, K. R.; Mukerji, I.; Spiro, T. G. *Science* **1995**, *269*, 1843.

(5) Hu, X.; Frei, H.; Spiro, T. G. *Biochemistry* **1996**, *35*, 13001.

(6) Hu, X.; Rodgers, K. R.; Mukerji, I.; Spiro, T. G. *Biochemistry* **1999**, *38*, 3462.

(7) Baldwin, J. M. *J. Mol. Biol.* **1980**, *136*, 103.

(8) Perutz, M. F. *Nature* **1970**, *228*, 726.

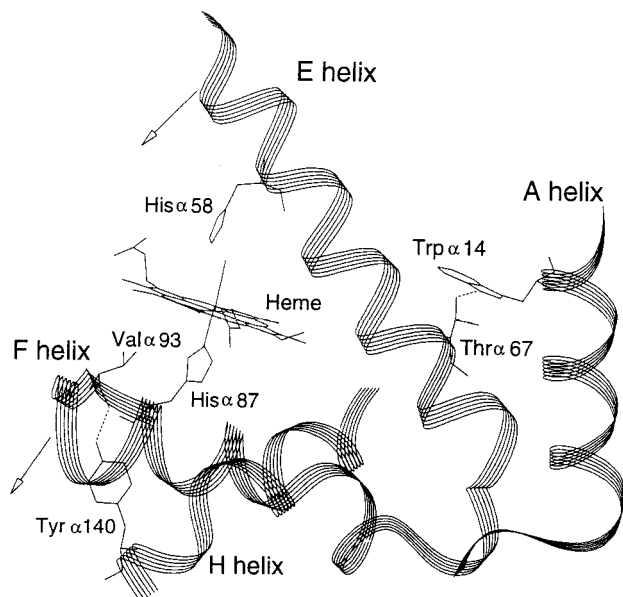


**Figure 1.** Diagram of the helix arrangement around the heme pocket of the  $\alpha$  chain of HbCO (PDB: 2HCO),<sup>7</sup> showing the H bond between Trp $\alpha$ 14 and Thr $\alpha$ 67, which bridges the A and E helices, and the H bond between Val $\alpha$ 93 and Tyr $\alpha$ 140, which bridges the FG corner and the H helix. The arrangements are similar for  $\beta$  chains, except that Trp $\beta$ 15 and Ser $\beta$ 72 provide the A–E bridge, whereas Val $\beta$ 98 and Tyr $\beta$ 145 bridge the FG corner and H helix. Also shown are the heme and the proximal and distal histidine residues ( $\alpha$ 87 and  $\alpha$ 58). The arrows indicate the direction of E, F helix displacements after photodeligation as proposed in the model of the allosteric coordinate.<sup>6</sup>

of H-bonds diminishes the Tyr and Trp intensities. This is what the time-resolved UVRR spectra show for the first intermediate after HbCO photolysis, which has a rise-time of  $\sim$ 50 ns and a decay time of  $\sim$ 500 ns.<sup>4,9</sup> The difference spectrum of the intermediate relative to unphotolyzed HbCO shows negative bands for both tyrosine and tryptophan.<sup>3,4</sup>

The same negative bands are seen when the UVRR spectra of tetra-ligated Hb is subtracted from that of any Hb construct in which one or more of the chains contain deoxy-heme, but whose quaternary structure remains R. These constructs include di-ligated Co, Fe hybrids,<sup>3</sup> tri-ligated cyanome-hybrids,<sup>10</sup> and Hb's for which the T state is destabilized by mutations,<sup>11</sup> or by C-terminal deletions.<sup>12</sup> This characteristic difference spectrum is labeled R<sub>deoxy</sub>. The loss of ligand within the R structure produces the same indications of H-bond weakening as are seen in the early intermediate in the HbCO photocycle. Significantly, the position of the tryptophan negative peaks, W3, distinguishes it as arising from Trp $\alpha$ 14 and  $\beta$ 15, and not the third residue, Trp $\beta$ 37, which is at the  $\alpha_1\beta_2$  interface, and forms a strong intersubunit H-bond only in the T state.<sup>2,13</sup>

Although suggestive, the negative peaks do not prove that H-bonds are involved. For this reason we have turned to site-directed mutagenesis, in hopes that the H-bonds under consideration can be eliminated without altering the protein fold. This hope is fulfilled in the Thr $\alpha$ 67 and Ser $\beta$ 72 mutants, for which we find no spectroscopically detectable disturbance of the

protein fold nor of the native T state intersubunit contacts. But the mutations do diminish the Trp $\alpha$ 14 and  $\beta$ 15 intensities, because of the loss in H-bonding. They also diminish the negative tryptophan peaks in the 150 ns time-resolved UVRR difference spectra, thereby establishing that these peaks do reflect loss of the E–A interhelical H-bonds.

## Materials and Methods

**Recombinant Hemoglobin (rHb) Expression and Purification.** pHE2 plasmid, in which synthetic human  $\alpha$ - and  $\beta$ -globin genes and the methionine aminopeptidase (Met-AP) gene from *Escherichia coli* are coexpressed under the control of separate *tac* promoters, was used to produce the rHb as well as its mutants.<sup>14</sup> The plasmids were transformed into *E. coli* JM109 or *E. coli* KS463, and protein was expressed following the procedures in ref 14.

Bacterial cells were stored frozen at  $-80$  °C until needed for purification and then thawed and sonicated twice in an ice bath. The membrane was centrifuged down (14 000 rpm, 45 min). The supernatant was saturated with CO gas, the pH was adjusted to 8.0 with Tris base, and a small volume (1.0 mL/L culture) of 10% polyethyleneimine (vol/vol) was added to precipitate most of the nucleic acids. The mixture was stirred for 15 min with a stream of CO gas blowing across the top and then centrifuged at 14 000 rpm for 45 min. The supernatant was concentrated in an Amicon stirred-cell concentrator at 4 °C.

Two columns were employed in the purification procedures. (a) A Q-Sepharose Fast-Flow column (Pharmacia anion exchanger) at 4 °C was used with a linear gradient of 20 mM Tris·HCl/0.5 mM triethylenetetramine (TETA), pH 8.3 to the same buffer with 160 mM NaCl; the flow rate was 5 mL/min. The buffer was exchanged by passing the samples through a G-25 (fine) column equilibrated with the beginning buffer. rHb remained at the top of the Q column, and the unwanted products including nucleic acids and other proteins were washed off with the beginning buffer. The rHb fraction was then eluted from the column in one major band by applying the linear gradient. (b) A Mono S column (Pharmacia cation exchanger HR16/10) at room temperature was used with a 10–30% gradient of 20 mM sodium phosphate/0.5 mM ethylenediaminetetraacetic acid (disodium salt) (EDTA), pH 8.3 (B), in 7.5 column volumes. The beginning buffer is 10 mM sodium phosphate/0.5 mM EDTA, pH 6.8 (A). The flow rate was 5 mL/min. A G-25 (fine) column was again employed to exchange the sample buffer to the initial buffer condition. The Hb met form was washed off the column in several peaks by elevating the gradient to 100% B. The Mono S column was controlled by an AKTA Purifier 10 HPLC system (Amersham Pharmacia). The elution profile of the expressed rHb usually gave multiple peaks, corresponding to different percentages of extra N-terminal methionine.<sup>14</sup> The relative intensity of these peaks varied depending on the *E. coli* strains, plasmids, and growing conditions. The last peak always has the least amount ( $\sim$ 0%) of the extra N-terminal methionine.

Past studies have shown that heme insertion into the  $\beta$  chain of rHb from the last peak is incorrect but the heme can be converted to the correct orientation by a simple oxidation–reduction process.<sup>14,15</sup> The converted rHb exhibits the same structural and functional properties as those of adult hemoglobin A (HbA). Therefore, all the rHb from the last peaks underwent the oxidation–reduction procedure.<sup>15</sup> No met form was found in the final product, as indicated by the absorption spectra. To confirm the absence of the met form, some samples were rechromatographed on the Mono S column, with the same linear gradient. No residual met peak was observed. The yield of pure protein from the last Mono S peak was  $\sim$ 10 mg/L culture.

**Site-Directed Mutagenesis.** In vitro mutagenesis was performed on the plasmid pHE2 using a Muta-Gene kit from BIORAD (catalog no. 170-3576). The strategy is shown in Scheme 1. Synthetic oligonucleotides 5'-GCAACAGCGTTAACCAGAGCATCAG-3' (25 mer) and 5'-AGACCGTCAGCGAAGCGCCAGAACTTTT-3' (30 mer) were used as primers to introduce the mutations  $\alpha$ 67 Thr  $\rightarrow$  Val and  $\beta$ 72

(9) Hofrichter, J.; Sommer, J. H.; Henry, E. R.; Eaton, W. A. *Proc. Natl. Acad. Sci. U.S.A.* **1983**, *80*, 2235.

(10) Jayaraman, V.; Spiro, T. G. *Biochemistry* **1995**, *34*, 4511.

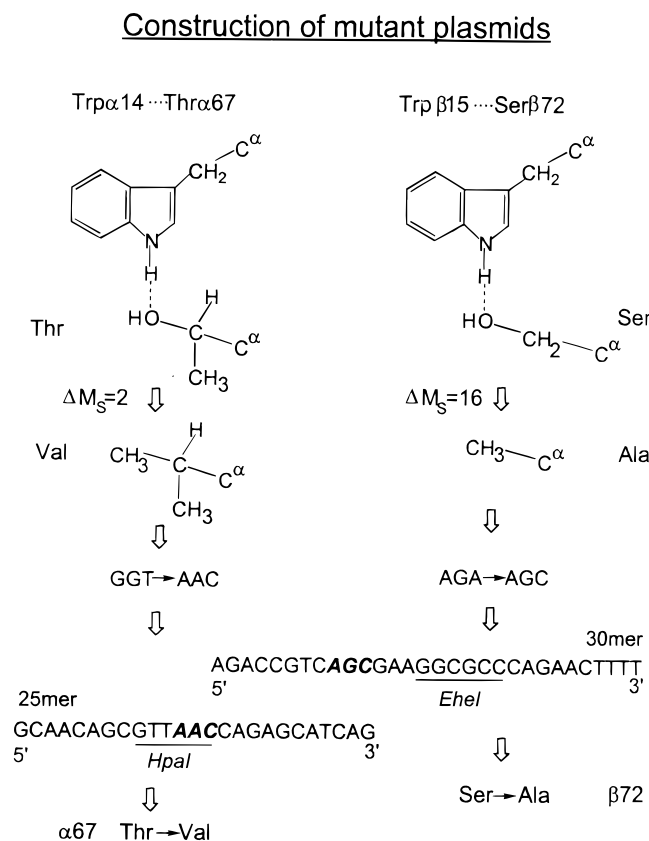
(11) Huang, J.; Juszczak, L. J.; Peterson, E. S.; Shannon, C. F.; Yang, M.; Huang, S.; Vidugiris, G. V.; Friedman, J. M. *Biochemistry* **1999**, *38*, 4514.

(12) Wang, D.; Spiro, T. G. *Biochemistry* **1998**, *37*, 9940.

(13) Nagai, M.; Kaminaka, S.; Ohba, Y.; Nagai, Y.; Mizutani, Y.; Kitagawa, T. *J. Biol. Chem.* **1995**, *270*, 1636.

(14) Shen, T. J.; Ho, N. T.; Simplaceanu, V.; Zou, M.; Green, B. N.; Tam, M. F.; Ho, C. *Proc. Natl. Acad. Sci. U.S.A.* **1993**, *90*, 8108.

(15) Sun, D. P.; Zou, M.; Ho, N. T.; Ho, C. *Biochemistry* **1997**, *36*, 6663.

**Scheme 1.** Scheme for the Construction of Mutant Plasmids for T $\alpha$ 67V and S $\beta$ 72A<sup>a</sup>

<sup>a</sup> A new *HpaI* restriction site was introduced by the new  $\alpha$  mutation codon, while a new *EheI* restriction site was purposely introduced into the  $\beta$  mutant. The codons shown in black are the mutated ones. Also shown are the expected mass differences between the wild-type and mutants.

**Table 1.** Electrospray Mass Spectrometry (ESMS) Masses (daltons)

	$\alpha$ chain	$\beta$ chain
HbA	15126.6	15867.6
rHb	15126.9	15867.9
T $\alpha$ 67V <sup>a</sup>	15124.8	15867.7
S $\beta$ 72A <sup>b</sup>	15127.0	15851.9

<sup>a</sup> The  $\beta$  chain mass is unaltered, while the  $\alpha$  chain mass is lowered by 2 amu, the expected difference between Thr and Val. <sup>b</sup> The  $\alpha$  chain mass is unaltered, while the  $\beta$  chain mass is lowered by 16 amu, the expected difference between Ser and Ala.

Ser  $\rightarrow$  Ala, respectively. A new *HpaI* restriction site was introduced into the  $\alpha$  mutant by the new codon. A new *EheI* restriction site was deliberately introduced into the  $\beta$  mutant by using the redundant codons for Gly69 (GGU  $\rightarrow$  GGC) and Ala 70 (GCU  $\rightarrow$  GCC). There are two *HpaI* sites and one *EheI* site in the native pHE2.

**Verification of Mutant Identities.** Mutated plasmids were initially checked by gel-electrophoresis of the products from the restriction enzyme (*HpaI* and *EheI*) digestions, and confirmed by DNA sequencing. The identities of the mutant proteins were confirmed by electrospray mass spectrometry (ESMS). The masses were exactly as expected (Table 1). The purity and homogeneity of the recombinant proteins were verified by polyacrylamide (10%) gel electrophoresis under both denaturing and nondenaturing conditions.

**Circular Dichroism.** Spectra were recorded on an Aviv model 62DS spectropolarimeter at 25 °C in a 1 mm path-length strain free quartz cell (111 QS, Hellma Cells Inc.) with 1.0 nm bandwidth, step size of 1 nm, and averaging time of two seconds for each data point. The spectra are the average of three scans. The samples were in 50 mM sodium phosphate pH 7.4 buffer. For near UV (180–320 nm) CD measure-

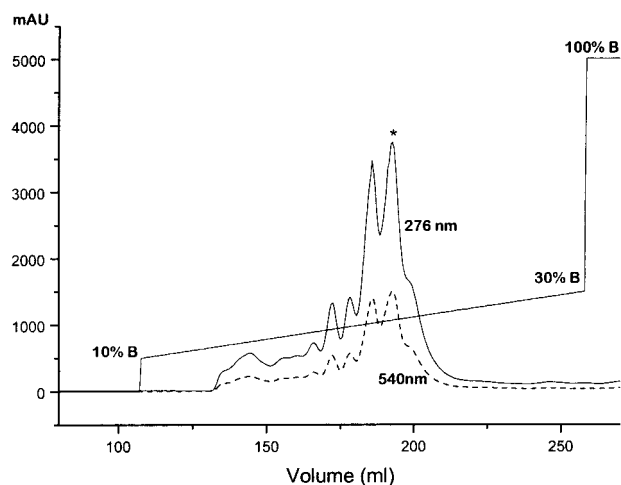


**Figure 2.** Elution profile of rHb from a Mono S column (HR 16/10) with a flow rate of 5 mL/min. Eluent A is 10 mM sodium phosphate/0.5 mM EDTA, pH 6.8, eluent B is 20 mM sodium phosphate/0.5 mM EDTA, pH 8.3, and the gradient is from 10% B to 30% B in 7.5 column volumes. The absorption at the two monitoring wavelengths (276 and 540 nm) are shown. The peak labeled with an asterisk was used for spectroscopic studies (see results).

ments, the  $A_{198}$  was adjusted to 0.8, while for heme CD (300–600 nm) measurements, the  $A_{419}$  was also 0.8. UV absorption spectra were recorded just before the CD experiments.

**Visible and UV Resonance Raman Spectroscopy.** The experimental setup has been described elsewhere.<sup>2,12</sup> Soret-resonant Raman spectra were obtained with a He–Cd laser (441.6 nm, Liconix) and a triple spectrograph (SPEX 1877) equipped with a 2400 groove/mm grating and intensified diode array detector (Princeton Instruments). The spectra were obtained in 20 min acquisitions. UVRR spectra were obtained with a frequency-doubled argon ion laser (229 nm, Coherent Innova 300) and a 1.26 m single spectrometer (SPEX) with an intensified diode array detector. Spectral acquisitions were carried out in 30 min increments. For time-resolved UVRR spectroscopy, a pair of Nd:YLF-pumped Ti:sapphire lasers provided  $\sim$ 25 ns pump (419 nm) and probe (229 nm) pulses at a 1 kHz repetition rate. The timing sequence alternated plus and minus time delays between the pump and probe lasers, and the accumulated pair of 10 min spectra were subtracted to produce a difference spectrum at the selected delay.<sup>16</sup> Final difference spectra were the average of 5–6 measurements.

Protein samples were 0.5 mM in heme, and were exchanged into 50 mM sodium phosphate (pH 7.4), 0.5 mM EDTA by centrifuging in buffer at least four times, using Centricon YM 30 (Millipore) tubes at 5000 rpm. 0.2 M NaClO<sub>4</sub> was used as the internal intensity standard to generate deoxy – CO UVRR difference spectra.

## Results

**Protein Expression and Purification.** Mono S chromatography of partially purified recombinant Hb reveals several Hb peaks (Figure 2), in addition to adventitious protein. The Hb peaks appear in the middle of the gradient and reflect differing contents of N-terminal methionine, as revealed by ESMS. The coexpressed methionine aminopeptidase is only partially effective at methionine cleavage of the recombinant Hb polypeptides.<sup>14</sup> The chromatographic pattern depends on the specific mutation and on the bacterial strain chosen for expression. We tried KS463 (not shown), as well as *E. coli* JM109 (Figure 2). The final peak in the gradient (marked with an asterisk) contains negligible amounts of extra methionine, as revealed by the mass spectrum, and has the same retention time as HbA. This fraction was used for spectroscopic characterization, following a redox

(16) Zhao, X.; Tengroth, C.; Chen, R.; Simpson, W. R.; Spiro, T. G. 1999, manuscript submitted.



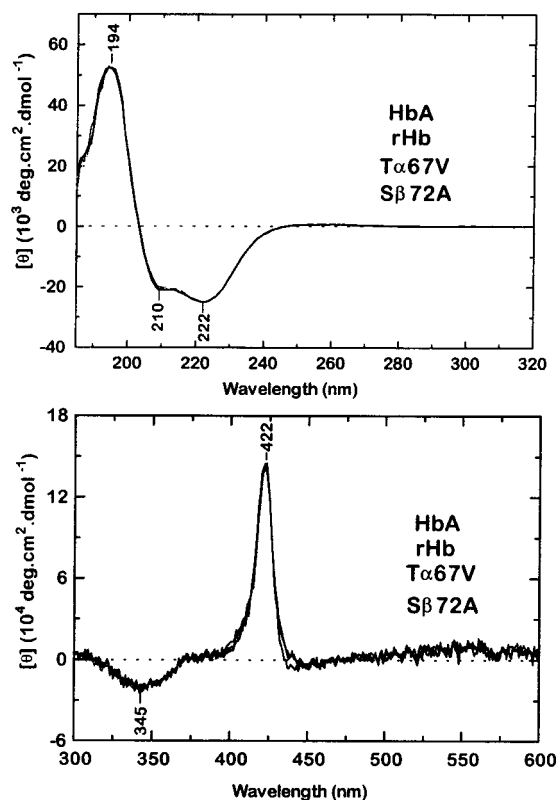


**Figure 3.** Circular dichroism spectra of the CO forms of recombinant wild-type and mutant Hb's, superimposed on those of HbA, in the UV (top) and visible (bottom) regions.

cycle (see Material and Methods) to ensure proper orientation of the inserted heme.

**Correct Folding and Quaternary Structure.** The bacterially expressed proteins were examined by circular dichroism to check for proper folding. Figure 3 shows that both mutants, as well as the unmutated recombinant Hb, have CD spectra identical with Hb A, at both ultraviolet and visible wavelengths. The signals at wavelengths below 250 nm reflect secondary structure,<sup>17</sup> and the conservation of negative band intensity at 210 and 222 nm ensures that the helical content is unaltered in the expressed proteins. At longer wavelengths, the CD signals are associated with the heme electronic transition and reflect chirality associated with electrostatic field of the surrounding protein.<sup>18</sup> The constancy of the CD bands seen at 345 and 422 nm ensures that the heme binding pockets are the same in all four proteins.

The status of the Fe–His bond, which connects the heme group to the protein, is also the same in the expressed proteins and in Hb A. The left panel of Figure 4 reveals identical frequencies and band shapes for the Fe–His resonance Raman band, obtained via excitation at 441.6 nm, in resonance with the heme Soret electronic transition. The band maximum, 215  $\text{cm}^{-1}$ , is characteristic of deoxyHb in the T state, as is the band shape. In deoxy-myoglobin, or in relaxed forms of deoxyHb, the Fe–His frequency is  $\sim 222 \text{ cm}^{-1}$ . Protein forces in the T state weaken the Fe–His bond, lowering its stretching frequency; the effect is greater in the  $\alpha$  than in the  $\beta$  chains, producing an asymmetric band shape.<sup>19–21</sup> Thus the 215  $\text{cm}^{-1}$  band maximum,

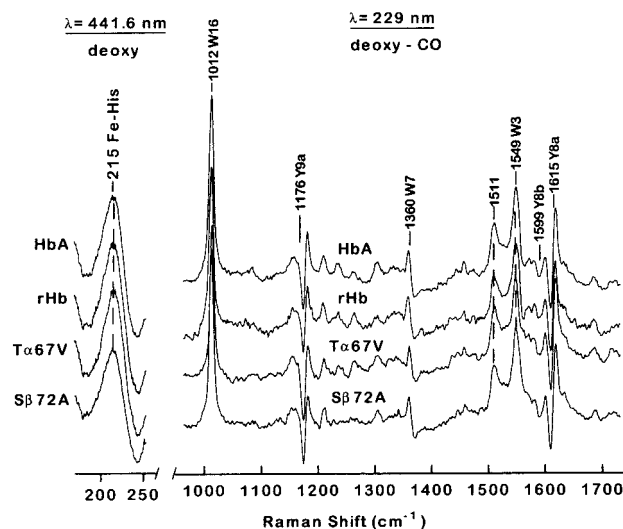


**Figure 4.** Comparison of visible RR spectra of deoxyHb excited at 441.6 nm (left panel) and UVRR difference spectra between deoxy and CO forms excited at 229 nm (right panel, W = Trp modes, Y = Tyr modes) (2) for HbA, rHb, and T $\alpha$ 67V and S $\beta$ 72A. The UVRR difference spectra are expanded by a factor of 3, relative to the parent spectra, and minor peaks (unlabeled) are not readily distinguishable from noise.

as well as the asymmetric shape, establish that the T state forces at the heme are the same in the expressed proteins as in Hb A.

Likewise the T state contacts in the  $\alpha_1\beta_2$  subunit interface are unaltered, as revealed by UVRR difference spectra between deoxyHb and HbCO, obtained with 229 nm excitation (Figure 4, right panel). These spectra<sup>2</sup> arise from environmental changes in tryptophan and tyrosine residues, and are dominated by two critical H-bonds, Tyr $\alpha$ 42 $\cdots$ Asp $\beta$ 99 and Trp $\beta$ 37 $\cdots$ Asp $\alpha$ 94, across the  $\alpha_1\beta_2$  interface, which are formed in the T state but are broken in the R state.<sup>1</sup> The key markers of these H-bonds are the sigmoidal Y8a (1615  $\text{cm}^{-1}$ ) band, which arises from an upshift in the T state frequency for Tyr $\alpha$ 42, and the W3 band position, 1549  $\text{cm}^{-1}$ , which arises from augmented intensity associated with Trp $\beta$ 37. The Trp $\beta$ 37 frequency is lower than that of the other two tryptophan residues, Trp $\alpha$ 14 and  $\beta$ 15, because of a lower dihedral angle about the bond connecting the indole ring to the C $\beta$  atom.<sup>2,22</sup>

Thus, the expressed proteins fold correctly, have unaltered heme pockets, and form proper T state contacts in deoxyHb.

**Signatures of H-bond Deletion.** When the UVRR spectrum of unmutated recombinant Hb is subtracted from those of the mutants (Figure 5), negative tryptophan signals are seen. The position of the negative W3 band is 1558  $\text{cm}^{-1}$ , characteristic of Trp $\alpha$ 14 and  $\beta$ 15, not 1548  $\text{cm}^{-1}$ , the Trp $\beta$ 37 position.<sup>2,23</sup> Thus, the intensity is unaltered for Trp $\beta$ 37 but is diminished for Trp $\alpha$ 14 or  $\beta$ 15. This intensity loss is attributable to the elimination of the H-bond partners of Trp $\alpha$ 14 or  $\beta$ 15. Importantly, the mutation-induced difference spectra are essentially the same for deoxyHb and for HbCO, establishing that the tertiary H-bonds do not differ between the T and R states.

However, the W3 intensity loss is greater for T $\alpha$ 67V than for S $\beta$ 72A; this is evident from inspection of the difference spectra. To quantify this effect, we deconvoluted the W3 band envelope in the parent spectra into contributions from Trp $\beta$ 37

(17) Yang, J. T.; Wu, C.-S. C.; Martinez, H. M. *Methods Enzymol.* **1986**, 130, 208.

(18) Chiancone, E.; Vecchini, P.; Verzili, D.; Ascoli, F.; Antonini, E. *J. Mol. Biol.* **1981**, 152, 577.

(19) Kitagawa, T. In *Biological Applications of Raman Spectroscopy*; Spiro, T. G., Ed.; John Wiley & Sons: New York, 1997; Vol. 3, pp 97.

(20) Nagai, K.; Kitagawa, T. *Proc. Natl. Acad. Sci. U.S.A.* **1980**, 77, 203.

(21) Mukerji, I.; Spiro, T. G. *Biochemistry* **1994**, 33, 13132.

(22) Miura, T.; Takeuchi, H.; Harada, I. *J. Raman Spectrosc.* **1989**, 20, 667.

(23) Hu, X.; Spiro, T. G. *Biochemistry* **1997**, 36, 15701.

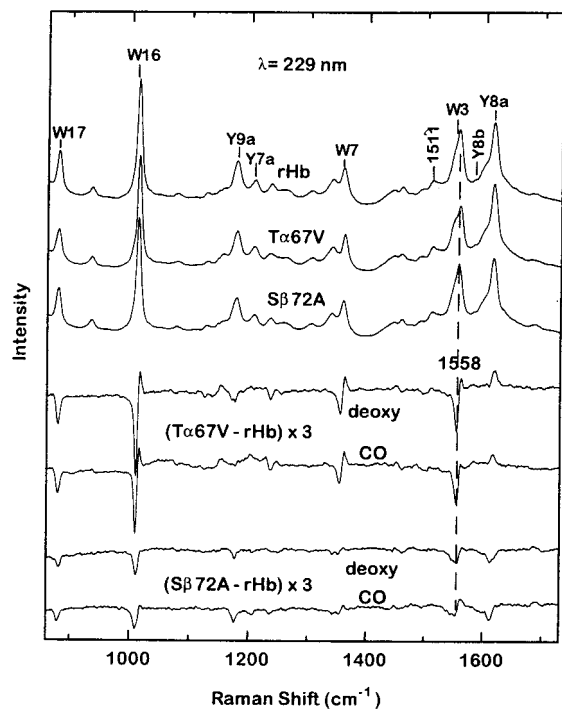


**Figure 5.** UVRr difference spectra ( $\times 3$  scale factor) between rHb and the two mutants, in deoxy and CO forms. Also shown are parent spectra of the deoxy forms.

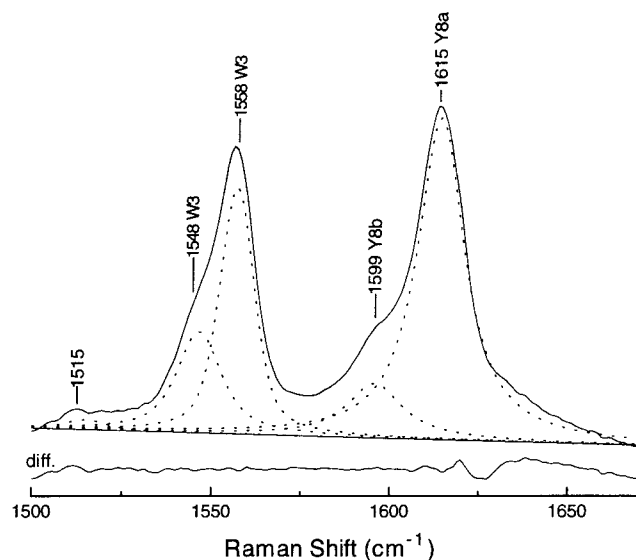


**Figure 6.** Illustration of the curve-fitting procedure used to extract the intensity of the W3 band components. The experimental data (solid trace) are compared with the curve-fit components with 50% Gaussian and 50% Lorentzian line shapes (dotted lines). The bottom trace is the difference between the experimental intensity and the sum of the fitted components.

(the  $1548\text{ cm}^{-1}$  shoulder) and from Trp $\alpha$ 14/ $\beta$ 15 (the  $1558\text{ cm}^{-1}$  main band) (Figure 6). The resulting intensities, expressed as Raman cross-sections, are given in Table 2. From the wild-type and mutant cross-sections we can evaluate the H-bond effects as follows:

$$4\sigma_{\text{WT}} = 4\sigma^0 + 2\sigma_{\alpha}^{\text{H}} + 2\sigma_{\beta}^{\text{H}} \quad (1)$$

$$4\sigma_{\text{T}\alpha 67\text{V}} = 4\sigma^0 + 2\sigma_{\beta}^{\text{H}} \quad (2)$$

$$4\sigma_{\text{S}\beta 72\text{A}} = 4\sigma^0 + 2\sigma_{\alpha}^{\text{H}} \quad (3)$$

**Table 2.** Raman Cross Section for the W3 Band at  $1558\text{ cm}^{-1}$  in the CO Adducts of Wild Type (WT) and Mutant Hb's (mbarn $\cdot$ molecule $^{-1}\cdot$ sr $^{-1}$ )<sup>a</sup>

	$\sigma$ (static)	$\sigma'$ (150 ns)
WT	1459	1218
T $\alpha$ 67V	1237	1132
S $\beta$ 72A	1332	1196
$\sigma^0$	1110	1110
$\sigma_{\alpha}^{\text{H}}$	444	172
$\sigma_{\beta}^{\text{H}}$	254	44
$\sigma_{\beta 37}(\text{T})^b$	1618	
$\sigma_{\beta 37}(\text{R})^b$	1142	

<sup>a</sup> Raman cross sections were calculated based on the peak-heights, which are a more reliable gauge of intensity than peak areas in complex spectra. ClO $_4^-$  was used as the internal intensity standard, and the cross section of its  $934\text{ cm}^{-1}$  peak,  $0.586\text{ mbarn}\cdot\text{molecule}^{-1}\cdot\text{sr}^{-1}$ <sup>24</sup> was used to calculate the W3 cross-sections from  $\sigma(\text{W3}) = (I_{\text{Trp}}/I_{\text{ClO}_4^-}) \cdot (C_{\text{ClO}_4^-}/C_{\text{Trp}}) \cdot \sigma_{\text{ClO}_4^-}$ . For the static spectra, the W3 intensities were determined by deconvoluting the W3/Y8a, Y8b region ( $1500\text{--}1670\text{ cm}^{-1}$ ) into five bands (Figure 6). Since there is no change for the W3 band at  $1548\text{ cm}^{-1}$  between the wild-type and mutant proteins, its peak width, height, and frequency were fixed. For the 150 ns cross section calculation, the difference spectra (Figure 7) were first normalized to the Y8a difference band as a secondary intensity standard to eliminate kinetic differences among the samples, as well as the effect of the slow build-up of met Hb during the measurements, as a result of exposure to the photolyzing laser. This Y8a correction factor set the static and time-resolved spectra to the same scale (defined by the magnitude of  $\sigma^0$ ) after the parent spectra of the 150 ns transient species were deconvoluted. <sup>b</sup> Cross section of the Trp $\beta$ 37 W3 peak at  $1548\text{ cm}^{-1}$  in HbCO ( $\sigma^{\text{R}}$ ) and deoxyHb ( $\sigma^{\text{T}}$ ), based on the same curvefitting procedures described above.

where  $\sigma_i$  is the cross-section per (interior) tryptophan for the indicated Hb species,  $\sigma^0$  is the average cross section of Trp $\alpha$ 14 and  $\beta$ 15, in the absence of any H-bond acceptor, and  $\sigma_{\alpha}^{\text{H}}$  and  $\sigma_{\beta}^{\text{H}}$  are the intensity increments due to the Trp $\alpha$ 14 and Trp $\beta$ 15 H-bonds, respectively. The assumption is that  $\sigma^0$  value is unaltered by the mutation and that neither Trp $\alpha$ 14 nor Trp $\beta$ 15 forms a H-bond with solvent water or with some other protein residue in the mutants. This assumption seems reasonable since the interhelical regions are protected from water, and since the mutations produce the same intensity loss in the R state as in the T state. We find that  $\sigma_{\alpha}^{\text{H}}$  and  $\sigma_{\beta}^{\text{H}}$  are 40 and 23% of  $\sigma^0$ , respectively. Thus, the tertiary H-bonds augment the intrinsic tryptophan intensity by about 20% for Trp $\beta$ 15 and by twice that amount for Trp $\alpha$ 14. For comparison, we measured the Trp $\beta$ 37 W3 cross-sections and obtained values of 1142 and 1618 mbarn $\cdot$ sr $^{-1}$  in HbCO and deoxyHb, respectively. The former value is within 3% of  $\sigma^0$ , indicating minimal enhancement from the weak intersubunit H-bond in the R state. The latter value is 42% higher, reflecting the strong quaternary H-bond in the T state (see below).

The mutations also perturb the tyrosine signals slightly but in different ways. T $\alpha$ 67V shows a positive Y8a difference band, while S $\beta$ 72A shows a negative one; both mutants have small negative difference signals for Y9a. The presence of three tyrosine residues on each chain makes interpretation of these signals uncertain, but we note that only the  $\beta$  chain has a tyrosine residue on the E helix, Tyr $\beta$ 130. This residue provides an additional A–E interhelical H-bond to the Val $\beta$ 11 carbonyl.<sup>12</sup> It is reasonable to infer that loss of the Trp $\beta$ 15 H-bond would also loosen the Tyr $\beta$ 130 H-bond, thereby producing a negative UVRr signal for Tyr as well as Trp.

**Time-Resolved RR Spectroscopy: E Helix Dynamics.** The effect of the mutations on 150 ns time-resolved difference spectra are shown in Figure 7. This time delay was chosen to isolate the spectrum of the first protein intermediate in the HbCO photocycle. This intermediate, called R $_{\text{deoxy}}$ , has a rise time of

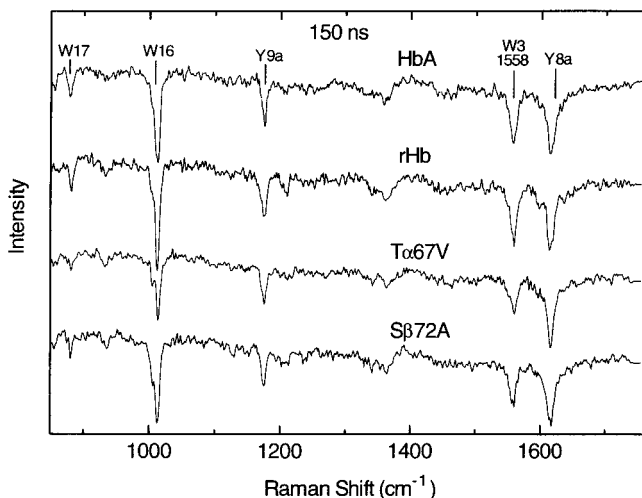


**Figure 7.** Pump-probe minus probe-pump UVRR difference spectra (pump = 419 nm, probe = 229 nm) at 150 ns time delay for CO forms of HbA, rHb, and T $\alpha$ 67V and S $\beta$ 72A. The scale factor is  $\times 3$ , and minor peaks (unlabeled) are not readily distinguishable from noise.

$\sim 50$  ns, and a decay time of  $\sim 500$  ns.<sup>4,9</sup> Its spectrum is characterized by diminished intensity in both tryptophan and tyrosine bands, and the position of the W3 difference band, 1558  $\text{cm}^{-1}$ , establishes Trp $\alpha$ 14 and  $\beta$ 15 to be the locus of the tryptophan intensity loss.<sup>2-4</sup> Figure 7 shows this early transient UVRR difference spectrum, recorded for a 150 ns delay, to be unaltered in recombinant Hb, showing the bacterially expressed protein to be the same as that in HbA in its dynamic as well as its static spectral indicators.

The mutants likewise show similar early transient difference spectra, but the tryptophan difference signals are diminished relative to those of tyrosine. Again we quantified this effect by deconvoluting the parent spectra into Trp $\beta$ 37 and Trp $\alpha$ 14/ $\beta$ 15 contributions (Table 2). As in the static spectra, we calculated the H-bond contributions using the equations

$$4\sigma_{\text{WT}}' = 4\sigma^{0r} + 2\sigma_{\alpha}^{\text{H}} + 2\sigma_{\beta}^{\text{H}} \quad (4)$$

$$4\sigma_{\text{T}\alpha 67\text{V}}' = 4\sigma^{0r} + 2\sigma_{\beta}^{\text{H}} \quad (5)$$

$$4\sigma_{\text{S}\beta 72\text{A}}' = 4\sigma^{0r} + 2\sigma_{\alpha}^{\text{H}} \quad (6)$$

where primes refer to the parent 150 ns time-resolved spectrum of Hb.  $\sigma^{0r}$  was set equal to  $\sigma^0$  via the scaling procedure (see the Table 2 footnote) which utilized the tyrosine Y8a difference band as a secondary intensity standard. This scaling serves to eliminate possible kinetic differences between native Hb and the mutants. The values  $\sigma_{\alpha}^{\text{H}} = 172$  and  $\sigma_{\beta}^{\text{H}} = 44$   $\text{mbarn}\cdot\text{molecule}^{-1}\cdot\text{sr}^{-1}$  are 61 and 83% smaller than the static increments  $\sigma_{\alpha}^{\text{H}}$  and  $\sigma_{\beta}^{\text{H}}$ . The interpretation of  $\sigma_{\alpha}^{\text{H}}$  and  $\sigma_{\beta}^{\text{H}}$  increments is model dependent, because at 150 ns, about half the CO molecules have recombined in native Hb, and it is not known whether the recombination is chain-selective or whether the protein structure is affected by the recombination at 150 ns. If, as seems likely, geminate recombination reverses the helix motions producing the R<sub>deoxy</sub> spectrum on the 150 ns time scale, then only the unligated chains contribute to the difference spectrum, and  $\sigma_{\alpha}^{\text{H}}$  and  $\sigma_{\beta}^{\text{H}}$  should be divided by the un-recombined fractions. This fraction is  $\sim 0.5$  for the tetramer, but it is not known how the recombined ligands are distributed between the  $\alpha$  and  $\beta$  chains. If recombination is equally probable in  $\alpha$  and  $\beta$  chains, then  $\sigma_{\alpha}^{\text{H}}$  and  $\sigma_{\beta}^{\text{H}}$  should be divided by 0.5

to estimate the H-bond increment per unligated chain. These divided values are 23 and 65% smaller than the static increments.

## Discussion

**Tertiary Trp H-bonding.** The T $\alpha$ 67V and S $\beta$ 72A mutants were prepared to evaluate tertiary H-bonds which we have proposed to play a key role in the allosteric transition from the R to the T state.<sup>3,4,6</sup> These H-bonds connect the N-terminal A helices, in both the  $\alpha$  and  $\beta$  chains, with the E helices, which line the distal side of the heme pockets (Figure 1). The indole rings of the A helix residues Trp $\alpha$ 14 and  $\beta$ 15 donate H-bonds to the hydroxyl groups of Thr $\alpha$ 67 and Ser $\beta$ 72. The residues chosen to replace Thr $\alpha$ 67 and Ser $\beta$ 72, Val and Ala, are sterically conservative (Scheme 1) but cannot form H-bonds. The mutated Hb's fold properly, as evidenced by the CD spectra in both the visible and UV region. Thus, the residue substitutions do not seriously diminish the stability of the native protein.

Furthermore, the disruption of the tertiary H-bonds is without significant impact on the quaternary interactions in the T state, as monitored by UVRR spectroscopy. The deoxyHb – HbCO difference UVRR spectra are the same for the mutants as for native Hb, showing that the intersubunit H-bonds across the  $\alpha_1\beta_2$  interface are unperturbed. Previous studies have shown that when these contacts are weakened, as in Hb constructs with C-terminal deletions<sup>12</sup> or in the Hb Kempsey (D99N) mutant,<sup>6</sup> the UVRR difference signals are attenuated. Thus, the intact deoxyHb – HbCO difference UVRR spectra establish that the quaternary structure is unaltered in the T $\alpha$ 67V and S $\beta$ 72A mutants.

When the indole ring is involved in a H-bond, the intensity of its 229 nm-excited UVRR scattering increases, because the H-bond lowers the energy of the resonant electronic transition and red-shifts the excitation profile.<sup>2</sup> The T $\alpha$ 67V and S $\beta$ 72A mutants serve to establish H-bond augmentation of the Trp $\alpha$ 14/ $\beta$ 15 UVRR intensity. The difference UVRR spectra between mutated and unmutated Hb show negative tryptophan bands, and the negative W3 peaks are at 1558  $\text{cm}^{-1}$ , the Trp $\alpha$ 14/ $\beta$ 15 position, which is 10  $\text{cm}^{-1}$  higher than the Trp $\beta$ 37 position. For each mutant, the magnitude of this negative W3 peak is the same whether deoxyHb or HbCO is evaluated, establishing that the Trp $\alpha$ 14 and  $\beta$ 15 H-bonds are equally strong in the T and the R state. This is the reason that the T – R difference spectrum has almost no intensity at the Trp $\alpha$ 14/ $\beta$ 15 position.

However the  $\alpha$  and  $\beta$  chain tertiary H-bonds differ from each other. The difference spectra reveal a greater intensity loss for T $\alpha$ 67V than for S $\beta$ 72A. Quantification of the W3 peaks reveals that the intensity augmentation is twice as large for the Trp $\alpha$ 14–Thr $\alpha$ 67 H-bond as for the Trp $\beta$ 15–Ser $\beta$ 72 H-bond. If the augmentation is assumed to be proportional to H-bond strength, then the Trp $\alpha$ 14 H-bond must be nearly twice as strong as the Trp $\beta$ 15 H-bond. This inference is supported by structural data (Table 3).<sup>25-27</sup> The X-ray coordinates yield significantly greater separation between the indole N atom and the O atom of the H-bond acceptor for Trp $\alpha$ 14 than for Trp $\beta$ 15. Taking the average of the deoxyHb and HbO<sub>2</sub> values, 2.68 and 3.20 Å, the separation is 0.5 Å greater for Trp $\beta$ 15. This increased separation could easily weaken the H-bond by a factor of 2. Thus, the two

(24) Dudik, J. M.; Johnson, C. R.; Asher, S. A. *J. Chem. Phys.* **1985**, *82*, 1732.

(25) Fermi, G.; Pertuz, M. F.; Shaanan, B.; Fourme, R. *J. Mol. Biol.* **1984**, *175*, 159.

(26) Tame, J.; Vallone, B. PDB: 1A3N, 1998.

(27) Shaanan, B. *J. Mol. Biol.* **1983**, *171*, 31.



**Table 3.** N···O Distance for Trp H-bonds<sup>a</sup>

		HbA		HbAO <sub>2</sub>
	partner	N···O (Å)	partner	N···O (Å)
Trpα14	Thrα67 (OH)	2.79 <sup>a</sup> /2.71 <sup>b</sup>	Thrα67 (OH)	2.60
Trpβ15	Serβ72 (OH)	3.11 <sup>a</sup> /2.88 <sup>b</sup>	Serβ72 (OH)	3.40
Trpβ37	Aspα94 (COO <sup>-</sup> )	2.99 <sup>a</sup> /2.90 <sup>b</sup>	Aspα94 (COO <sup>-</sup> )	3.57

<sup>a</sup> Calculated from the single-crystal X-ray coordinates in the Brookhaven Protein Data Bank of HbA ( $a = 1.74$  Å, PDB: 2HHB;<sup>25</sup>  $b = 1.80$  Å, PDB: 1A3N<sup>26</sup>) and HbAO<sub>2</sub> (2.1 Å, PDB: 1HHO<sup>27</sup>) using the program Insight II.

tertiary H-bonds, although symmetrically positioned in the αβ dimer, are not equally strong.

The H-bond augmentation of Trpα14 is almost as large as it is for Trpβ37 in the T state. The Trpβ37 W3 cross-section in the R state (Table 2) is essentially the same as the intrinsic, non-H-bonded intensity calculated for Trpα14 and Trpβ15 from the mutant spectra. This is consistent with the long N···O distance, 3.57 Å, obtained from the X-ray coordinates (Table 3), implying a very weak (or no) H-bond between Trpβ37 and the carboxylate side chain of Aspα94. In the T state, the intensity increases by 42%, reflecting the strong H-bond formed with Aspα94. Although the N···O distance, 2.95 Å, is intermediate between the tertiary H-bond distances for Trpα14 and Trpβ15 (Table 3), a strong H-bond is consistent with the anionic character of the H-bond acceptor for Trpβ37. Other environmental factors may also contribute to the intensity but are unlikely to explain the Trpβ37 intensification in the T state since examination of the crystal structures shows that the disposition of the surrounding residues, other than the H-bond acceptor, is essentially the same in the R and T states.

**E Helix Displacement in the R<sub>deoxy</sub> Structure.** Time-resolved UVRR spectroscopy of the Tα67V and Sβ72A mutants provides a direct support for the hypothesis that the initial step along the R–T allosteric reaction coordinate includes displacement of the E helix toward the heme and away from the outer A helix (Figure 1). The interhelical H-bonds formed by Trpα14 and β15 serve to monitor this displacement via the loss in UVRR intensity when the H-bonds are weakened.<sup>3</sup> The time-resolved UVRR spectra of the mutants confirm the H-bond origin of this intensity loss since the negative W3 difference band is decreased in intensity when either H-bond acceptor, Thrα67 or Serβ72, is mutated.

Quantification of the W3 intensities in the 150 ns time-resolved spectra (Table 2) establishes the H-bond contributions to the Trpα14 and β15 intensity losses in the R<sub>deoxy</sub> intermediate. The increments attributed to H-bonding,  $\sigma_{\alpha}^{\text{H}}$  and  $\sigma_{\beta}^{\text{H}}$ , are much lower than in the static spectrum, but interpretation of their magnitude is complicated by the unknown effects of geminate recombination, which occurs in about half the chains on average. It seems likely that recombination quickly (<150 ns) reverses the early structural effects of deligation, and that  $\sigma_{\alpha}^{\text{H}}$  and  $\sigma_{\beta}^{\text{H}}$  should be divided by the fraction of chains that have not recombined. The fraction is about 0.5 for the Hb tetramer, implying that  $\sigma_{\alpha}^{\text{H}}$  and  $\sigma_{\beta}^{\text{H}}$  should be doubled, if recombination is equally probable for α and β chains. The doubled values are 23 and 65% smaller than the static increments  $\sigma_{\alpha}^{\text{H}}$  and  $\sigma_{\beta}^{\text{H}}$ ,

respectively. The implication is that the stronger Trpα14 is weakened only modestly, while the weaker Trpβ15 H-bond is weakened substantially. However, the results would be altered if recombination were biased toward α or β chains. For example, if the recombination yield were 0.25 for α chains and 0.75 for β chains, then the H-bond increments, per unligated chain, would be 48 and 31% smaller, respectively, than  $\sigma_{\alpha}^{\text{H}}$  and  $\sigma_{\beta}^{\text{H}}$ , thus reversing the relative extent of the implied H-bond weakening. However, complete chain selectivity is ruled out by our results since either  $\sigma_{\alpha}^{\text{H}}$  or  $\sigma_{\beta}^{\text{H}}$  would then be zero, that is, the wild-type R<sub>deoxy</sub> difference spectrum would be unaltered for one or the other of the mutants.

Regardless of the quantitative uncertainty about the extent of H-bond weakening, the mutant spectra provide support for our model of the R–T allosteric coordinate, in which the R<sub>deoxy</sub> intermediate is formed via a rotation of the EF “clamshell” (Figure 1), in response to steric forces generated by de-ligation.<sup>6</sup> When the Fe–CO bond is broken, the Fe atom moves out of the heme plane, pushing on the F helix, while departure of the CO from the heme pocket permits collapse of the distal E helix toward the heme. The helix displacements are proposed to be concerted, ~50 ns being the characteristic time for the clamshell rotation. Interestingly, just such a rotation has recently been identified as the principle structural change between deoxy- and CO-myoglobin when the crystal structures are solved at ultrahigh resolution (1.15 Å).<sup>28</sup> The rotation angle is 1.7° in myoglobin, resulting in backbone displacements of 0.3–0.4 Å near the proximal and distal histidine residues. Displacements of this magnitude would be sufficient to weaken interhelical H-bonds substantially.

The loss in interhelix H-bonding is energetically costly and is driven by the photochemical deligation. In our model of the allosteric coordinate,<sup>6</sup> the next step involves re-formation of these H-bonds via following motions of the outer helices, A and H. The evidence for this proposal is that the negative peaks of the R<sub>deoxy</sub> difference spectrum disappear as the next intermediate, S, is formed, on the 500 ns time scale. The A and H helices contain the N and C termini of the polypeptide chain, which form intersubunit salt-bridges that stabilize the T state.<sup>8,12</sup> The docking of these salt-bridges is proposed to be the final, 20 μs step on the allosteric coordinate. Thus the pathway from the R to the T state is suggested to proceed via reciprocating helix motions which are initiated by de-ligation forces, mediated by interhelical H-bonds, and terminated by intersubunit salt-bridge formation. The present result supports this model by confirming the involvement of two of the inter-helical H-bonds.

**Acknowledgment.** We thank Mr. Greg D. Bowman for facilitating the usage of the micorferm fermentor and Dr. Xinshan Kan for the help with CD measurements. The ESMS measurements were performed in the electrospray mass spectrometry facilities at Princeton University (NIH IS10RRO). This work was supported by NIH grants GM25158 (to T.G.S.) and HL24525 (to C.H.).

JA992228W

(28) Kachalova, G.; Popov, A. N.; Bartunik, H. D. *Science* **1999**, *284*, 473.